

Effect of sepiolite on the physical properties and swelling behavior of rifampicin-loaded nanocomposite hydrogels

A. L. Viçosa^{1,2}, A. C. O. Gomes¹, B. G. Soares¹, C. M. Paranhos^{3*}

¹Instituto de Macromoléculas, Universidade Federal do Rio de Janeiro, Centro de Tecnologia, Av. Horacio Macedo 2030, Bloco J, Ilha do Fundão, 21945-598, Rio de Janeiro – RJ, Brazil

²Laboratório de Tecnologia Farmacêutica, Complexo Tecnológico de Medicamentos, Fundação Oswaldo Cruz, Av. Comandante Guarany 447, Jacarepagua, 21041-250, Rio de Janeiro – RJ, Brazil

³Laboratório de Permeação e Sorção, Departamento de Engenharia de Materiais, Universidade Federal de São Carlos, Rod. Washington Luiz, km 235, 13565-905, São Carlos – SP, Brazil

Received 28 March 2009; accepted in revised form 25 May 2009

Abstract. Nanocomposite hydrogels based on poly(vinyl alcohol) – PVA and sepiolite have been prepared and their potential for drug delivery systems has been assessed by taking rifampicin as model drug. The nanocomposite hydrogels were characterized by WAXS and DSC and the swelling behavior and structural stability were evaluated. The effect of the presence of rifampicin, sepiolite and simultaneous rifampicin-sepiolite on the structure and swelling of the hydrogels was investigated. The swelling data were analyzed in order to evaluate the diffusion mechanisms of water. The results indicate that both rifampicin and sepiolite cause important modifications on microstructure of the PVA matrix, leading to changes on swelling and diffusional behavior.

Keywords: polymer gels, poly(vinyl alcohol), hydrogel, nanocomposite, rifampicin

1. Introduction

Recent epidemiologic data report a strong growing up of tuberculosis in several countries. World Health Organization (WHO) indicates that about one third of world population is infected by *Mycobacterium tuberculosis* [1]. Among several reasons, the blowing up of AIDS cases, low nutritional and immunologic level of several parts of world, bacterial resistance caused by partial treatment and the inadequate bioavailability of the current pharmaceutical forms play an important role on this neglected epidemic [2].

In order to minimize the bacterial resistance and enhance the adherence to the treatment by the patients, the Center of Disease Control (CDC), the International Union Against Tuberculosis and Lung

Disease (IUATLD) and WHO have recommended the use of fixed dose combination (FDC). Tuberculosis treatment preconized by WHO involves the use of rifampicin, isoniazid, pirazinamide and ethambutol for a period of 6 months. However, FDC's are effective in tuberculosis treatment if correctly dosed in blood plasma [3]. Rifampicin is a class II drug (low solubility and high permeability) of biopharmaceutics classification system (BCS) and is well known for its poor solubility in water and bioavailability problems [4]. Figure 1 shows the chemical structure of rifampicin.

In order to enhance the solubility and bioavailability of poorly water-soluble hydrophobic drugs as rifampicin, several methods have been employed: decreasing of particle size and the crystallinity of

*Corresponding author, e-mail: caiomp.dema@gmail.com
© BME-PT

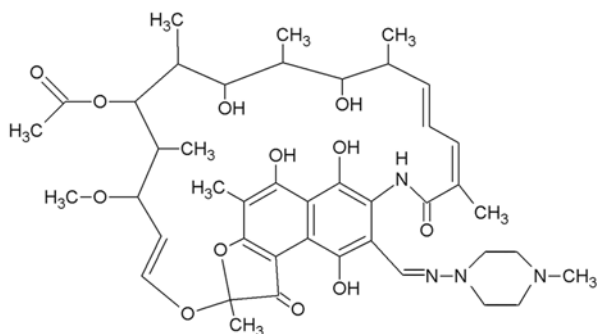


Figure 1. Chemical structure of rifampicin

the drug and/or using a carrier with high specific surface area. The adsorption of the drug onto a high surface area carrier is an interesting technique to modify the dissolution profile of rifampicin. It is well known that inorganic species can be used in order to improve the dissolution rate of drugs. Monkhouse and Lach (1972) were the first to report the use of silica in order to improve the dissolution rate of several drugs, including chloramphenicol, aspirin and indomethacin [5, 6]. It was observed that smectite increases the dissolution rate of non-ionic drugs due the hydrophilic nature of the clay [7, 8]. Recently, Aguzzi and co-authors published a comprehensive review of the use of clay minerals as drug delivery systems [9].

We have utilized natural sepiolite in order to improve the dissolution rate of rifampicin. Sepiolite is a fibrous clay mineral with fine microporous channels of dimensions 0.37×1.06 nm running parallel to the length of fibers. Typically, sepiolite shows an average size of $800 \times 25 \times 4$ nm, resulting in a material with an external surface area of the same order of magnitude as the area of macroporous. The structure of sepiolite, in some aspects, is similar to zeolites [10]. The presence of structural tunnels and blocks together with the fine particle size and the fibrous nature explain the high specific surface area present in sepiolite. Nevertheless, the use of sepiolite in order to improve the dissolution rate of poorly water-soluble drugs is still inadequately studied. However, changes on the microstructure of the polymeric matrix due the simultaneous presence of the clay and the drug must be predicted in order to avoid misinterpretation of the obtained results.

In the present investigation hydrogels based on poly(vinyl alcohol) (PVA) and sepiolite were prepared and loaded with rifampicin. The effect of the presence of sepiolite and rifampicin on the physical

properties and swelling behavior of the hydrogels was studied.

2. Materials and methods

2.1. Materials

Poly(vinyl alcohol), degree of hydrolysis 99%, $M_w = 120\,000$, was purchased by Sigma. Natural sepiolite was purchased by Fluka. Rifampicin was kindly supplied by Najiegun Pharmaceutical, China. All materials were used without further purification.

2.2. Preparation of hydrogels

An appropriate amount of clay was stirred in distilled water at room temperature for 1 h, followed by mechanical stirring during 30 min. To the resulting suspension, 5 g of PVA and 0.025 g of sodium benzoate (a multi-purpose preservative) were added and the suspension was heated under reflux at 95°C for 4 h under stirring. Rifampicin was previously dispersed in polysorbate (Tween 80 – Vetec). Recently, Mehta and collaborators reported the use of Tween 80 in order to increase the solubility of rifampicin in water [11]. After the reflux time, PVA solution was cooled until 40°C . Then, rifampicin was added and the final suspension was stirred with an Ultra Turrax homogenizer (IKA) during 10 min at 6500 rpm. Table 1 shows the sample designation of the obtained hydrogels. The suspension was poured in Petri dishes and maintained in a refrigerator at $8\text{--}10^\circ\text{C}$ for 24 h in order to form stable hydrogels.

Table 1. Composition and designation of nanocomposite hydrogels

| Sample designation | PVA [wt%] | Sepiolite [wt%] | Rifampicin |
|--------------------|-----------|-----------------|------------|
| PVA | 100 | – | – |
| PVAR | 100 | – | 150 mg |
| PVAS1 | 99 | 1 | – |
| PVAS5 | 95 | 5 | – |
| PVAS1R | 99 | 1 | 150 mg |
| PVAS5R | 95 | 5 | 150 mg |

2.3. Swelling behavior

The hydrogels matrices were allowed to swell in pH 7.4 phosphate saline buffer solution (PBS) at 30°C for 24 h. At predetermined time intervals, the

weight of the hydrogels was checked in an electronic balance after wiping the hydrogel surface with a filter paper. The swelling ratio, S , was then calculated from Equation (1):

$$S = \frac{W_s - W_d}{W_d} \quad (1)$$

where W_s and W_d are the swollen and the dry weight of the hydrogel, respectively. The average standard deviation was set in 10%.

2.4. Samples characterization

Wide-angle X-ray scattering (WAXS) was performed in a Rigaku Miniflex in a 2θ range of $2\text{--}40^\circ$ at room temperature, operating under a $\text{CuK}\alpha$ radiation ($\lambda = 1.5405 \text{ \AA}$). Thermal analyses were assessed by a Perkin-Elmer DSC-7. All measurements were made at a scan rate of $10^\circ\text{C}/\text{min}$, in the temperature range of 40 to 250°C , under continuous nitrogen gas flow. The structural stability of the samples was evaluated spectrometrically. The amount of PVA released from the hydrogels samples was determined by immersing small pieces of the hydrogels in distilled/deionized water. Then, after pre-established times (1, 2, 8 and 24 h) an aliquot of 10 ml of the releasing solution was removed and replaced with the same amount of fresh distilled water. The aliquot was then treated with a 0.65 M boric acid solution and a 0.05 M $\text{I}_2/0.15 \text{ M KI}$ solution. It is well known that PVA and boric acid/iodine complexes, resulting in a green complex [12]. The absorbance of visible light at 670 nm was then measured in a Cary 100 (Varian) UV-Visible spectrophotometer.

3. Results and discussion

The WAXS patterns of the hydrogels are shown in Figure 2. The strong diffraction peak observed at $2\theta = 7.5^\circ$ for sepiolite is related to the (110) crystallographic plane. This plane corresponds to the zeolitic pore inside the sepiolite needles that cannot be modified by chemical modifications or preparation from solution [13]. Unfortunately, it is not possible to calculate the degree of crystallinity of the samples containing sepiolite, since the $2\theta = 19.75^\circ$ and 20.65° (060 and 131 reflections, respectively [14]) of sepiolite overlaps the 101 and $10\bar{1}$ reflec-

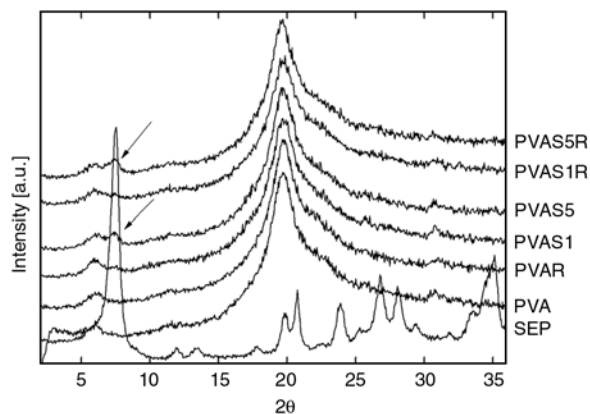


Figure 2. WAXS patterns of nanocomposite hydrogels. The curves are vertically offset for clarity.

tions of PVA ($2\theta = 19.5$ and 20.1° , respectively). Therefore, WAXS results will be used to evaluate possible changes on the crystalline structure of PVA.

At first glance, the presence of rifampicin and sepiolite do not cause significant change on the monoclinic crystal of PVA. The strong reflection at $2\theta = 19.6^\circ$ (plane 101 of PVA) does not show significant shifts with the presence of both sepiolite and rifampicin, indicating that no preferential crystalline orientation or constriction was detected. Despite the several reflections peaks observed in pure rifampicin (not shown), WAXS results of the PVAR sample do not show any evidence of crystalline reflections associated to rifampicin. Thus, the content of rifampicin added in the PVA matrix was not able to cause significant changes on the monoclinic crystal of PVA. It is known that the presence of lamella-type phyllosilicates, as montmorillonite, causes significant changes on the crystalline structure of several polymers [15, 16]. This fact is mainly caused by the confining crystallization environment provided by the clay platelets. On the other hand, the high aspect ratio of sepiolite fibers leads to a less confinement effect, resulting in a stable PVA crystallite. This behavior is consistent with observed to the samples PVAS1 and PVAS1R. However, for the samples containing 5% of sepiolite (PVAS5 and PVAS5R) it is possible to observe a relative small reflection corresponding to the 110 plane of sepiolite. These features indicate that higher content of sepiolite leads to the agglomeration of the sepiolite fibers. Similar behavior was reported by Chen and co-authors to sepiolite/polyurethane nanocomposites [17].

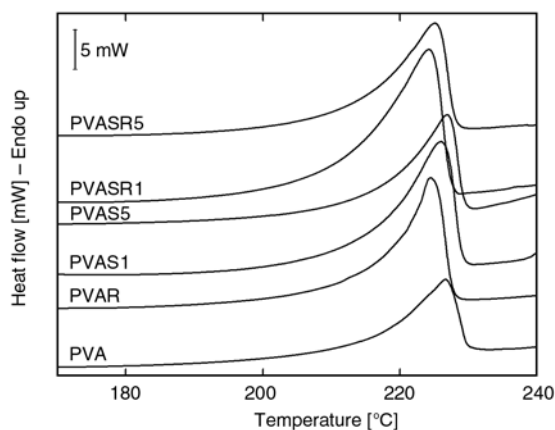


Figure 3. DSC curves of nanocomposite hydrogels. The curves are vertically offset for clarity.

In order to evaluate the crystalline nature of the hydrogels, the influence of sepiolite and rifampicin on the crystallinity of PVA matrix was also evaluated by DSC. Figure 3 presents the DSC heating curves and the Table 2 summarizes the crystalline melting parameters for the PVA-based samples. Pure PVA exhibits an endothermic peak at 227°C, corresponding to the crystalline melting point (T_m) of PVA. The presence of rifampicin causes a slight shifting of the melting peak of PVA to lower temperatures. This effect is attributed to the interactions between PVA and rifampicin and its large molecular size ($M_w = 823$). PVA hydroxyl groups can interact via hydrogen bonding with rifampicin. As can be seen in Figure 1 rifampicin has a lot of functional groups that can create hydrogen bonding [18]. These interactions together the large molecular size cause some disruption of the lamellar arrangement of the crystalline domains of PVA, consequently leading to lower T_m [19]. Table 2 shows that ΔT and fwhm (full-width half-maxi-

Table 2. Thermal parameters of nanocomposite hydrogels obtained by DSC*

| Sample | T_m [°C] | T_{onset} [°C] | ΔT^a | fwhm ^b | X_c [%] |
|--------|------------|------------------|--------------|-------------------|-----------|
| PVA | 226.6 | 215.0 | 11.6 | 7.8 | 37.3 |
| PVAR | 224.2 | 218.1 | 6.1 | 6.7 | 43.4 |
| PVAS1 | 226.0 | 215.0 | 11.0 | 8.0 | 36.3 |
| PVAS5 | 226.8 | 217.4 | 9.4 | 7.2 | 51.4 |
| PVAS1R | 224.2 | 210.8 | 13.4 | 9.3 | 44.6 |
| PVAS5R | 224.8 | 213.5 | 11.3 | 8.6 | 42.2 |

*The experimental errors associated with the thermal analysis experiments are $\pm 0.8^\circ\text{C}$ and $\pm 1.5\%$ for T_m and X_c , respectively.

^a $\Delta T = T_m - T_{onset}$

^bfwhm = full width at half maximum

^c X_c is calculated by the ratio of $\Delta H/\Delta H_m^0$, where ΔH_m^0 is the melting enthalpy of 100% crystalline PVA, i.e. 150 J/g [20].

mum) decrease by the addition of rifampicin on PVA matrix, indicating simultaneous increases in the rate of melting and the average crystalline size. Rifampicin shows its melting followed by recrystallization and decomposition in the range of 180–223°C and 247–266°C, respectively [20]. Unfortunately, the melting temperature of PVA is located at the same range. Nevertheless, no evidence of both processes of rifampicin was observed in DSC curves. It seems that rifampicin undergoes an amorphization process during the preparation of the hydrogels. Schierholz has reported a similar effect in shunts based on poly(dimethylsiloxane) loaded with 0.5–10% (w/w) of rifampicin [21]. Therefore, rifampicin acts as nucleating agent for PVA, resulting in less ordered crystalline domains and higher degree of crystallinity when compared to the pure PVA. The same behavior is observed to PVAS1R and PVAS5R, confirming the strong interaction between rifampicin and PVA. However, the monoclinic crystal of PVA does not undergo significant changes as can be seen in WAXS patterns. As a fact, the microstructure of PVA hydrogels is formed by a bicontinuous structure with a PVA-rich phase (crystalline domains) and a PVA-poor phase (amorphous domains) [22]. Thus, the DSC results reflect the changes on the crystalline domains which correspond to the PVA-rich phase. In concordance with the WAXS results, the presence of sepiolite does not cause changes in T_m of the samples PVAS1 and PVAS5.

The dispersion state of sepiolite can be evaluated by changes on degree of crystallinity (X_c) of the samples PVAS1 and PVAS5. The highly dispersed state of sepiolite fibers in PVAS1 can be confirmed, since no changes occur in the crystalline parameters listed in Table 2 when compared with pure PVA. However, the presence of 5% of sepiolite has a nucleating effect on the PVA matrix. Similar results were recently reported by Ma and collaborators for polypropylene/sepiolite nanocomposites [23]. The thermal parameters of PVAS1R and PVAS5R samples reveal a clear evidence that rifampicin plays a key role in the formation of the crystalline domains of PVA. Even with increasing amounts of sepiolite, the crystalline parameters of the samples tend to follow the behavior showed to PVAR sample. It is important to note that the addition of rifampicin was realized after the incorporation of the clay, as can be seen in Section 2.2.

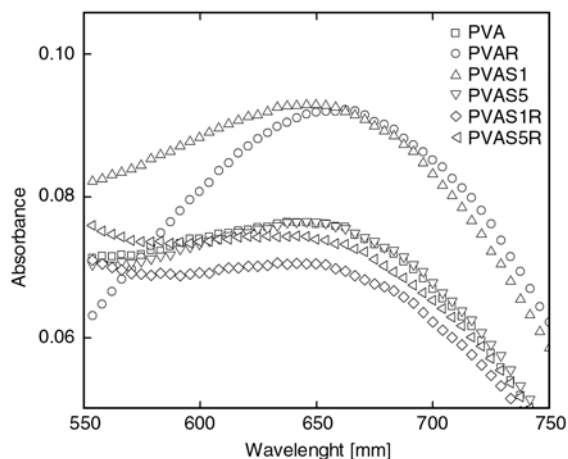


Figure 4. UV-Vis spectra of nanocomposite hydrogels after 24 h immersed in PBS

Therefore, the presence of rifampicin affects directly the final crystalline domains of PVA.

The results of the structural stability of the PVA matrix after 24 h immersed in PBS were evaluated spectrometrically, as can be seen in Figure 4. It is possible to note that all formulations containing sepiolite contribute to stabilize the residual PVA chains, except for PVAS1 sample. The presence of rifampicin results in an increasing number of PVA chains that does not contribute to form new crystallites, resulting in less ordered crystallites. This is consistent with the DSC results. It seems that the presence of sepiolite tends to prevent the diffusion of the residual PVA chains through the hydrogel. Since the presence of sepiolite does not impede the crystalline disorder caused by rifampicin, it is reasonable to expect that residual PVA chains are readily linked with sepiolite fibers. The case of PVAS1 sample is quite different, presenting the same amount of residual PVA chains observed to PVAR. This trend is consistent with a highly dispersed state of sepiolite. Since the average distance between clay fibers is considerable, it is expected that the intensity of the interactions between PVA and sepiolite is diminished; therefore the presence of small amounts of sepiolite do not contribute to retain the residual PVA chains.

Swelling behavior is an important parameter to characterize the hydrogels because it has a significant influence on the process of controlled release of drugs [24]. The swelling ratios as a function of the time for the hydrogels in PBS are shown in Figure 5. It is possible to note that the presence of sepiolite causes a decrease in the swelling capacities of

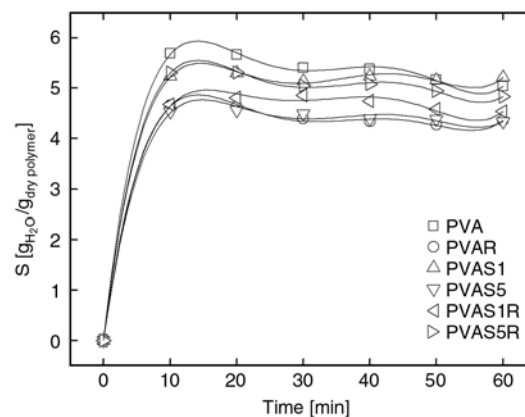


Figure 5. Swelling ratio of nanocomposite hydrogels in pH 7.4 at 30°C

the hydrogels when compared to pure PVA. The highly dispersed clay causes a decrease in available free volume of the PVA matrix, leading to lower swelling ratio. In the case of PVAS5, increase on X_c also contributes to diminish the available free volume for water diffusion. PVAR shows similar low degree of swelling when compared to PVAS5. However, PVAR has lowest X_c observed between the samples. This fact indicates that the presence of amorphized rifampicin leads to an obstruction effect, therefore reducing the number of pores available for water diffusion into the matrix. This effect is simultaneous with the increase of X_c in PVAR samples.

The dynamics of water sorption process was studied by monitoring the water imbibed by the hydrogels using Equation (2) [25]:

$$\frac{W_t}{W_\infty} = Kt^n \quad (2)$$

where W_t and W_∞ is the weight of swollen hydrogel at time t and at infinitely equilibrium swollen state, respectively, K is a characteristic constant and n is a characteristic exponent of the mode transport of the water. According to the classification of the diffusion mechanism, $n = 0.5$ indicates a quasi-Fickian diffusion; for $1/2 < n < 1$ anomalous, non-Fickian diffusion model operates and for $n = 1$ occurs a non-Fickian case II mechanism [25]. Table 3 summarizes the diffusion parameters of the PVA-based hydrogels. The obtained data indicate that the swelling transport mechanism is consistent with a quasi-Fickian process. This feature reveals a simultaneous contribution of the random mobility of water molecules into the PVA matrix and the solva-

Table 3. Transport properties of nanocomposite hydrogels

| Sample | Diffusion exponent (n) | Kinetic constant (K) | Correlation coefficient (r ²) | Diffusion coefficient [cm ² /s]·10 ⁸ |
|--------|------------------------|----------------------|---|--|
| PVA | 0.52 | 0.040 | 0.996 | 1.48 |
| PVAR | 0.47 | 0.052 | 0.994 | 1.75 |
| PVAS1 | 0.51 | 0.330 | 0.996 | 1.25 |
| PVAS5 | 0.46 | 0.420 | 0.993 | 4.79 |
| PVAS1R | 0.51 | 0.340 | 0.994 | 2.03 |
| PVAS5R | 0.48 | 2.920 | 0.996 | 2.34 |

tion of the high hydrophilic groups of PVA chains. The following model (Equation (3)) was used to calculate the diffusion coefficient, D , for $W_t/W_\infty \leq 0.8$ [25]:

$$\frac{W_t}{W_\infty} = 4 \left(\frac{Dt}{\pi l} \right)^{0.5} \quad (3)$$

where l is the initial thickness of the hydrogel. The calculated diffusion coefficients are shown in Table 3. Since the degree of crystallinity of PVAR is higher than pure PVA, increase of diffusion coefficient of PVAR can be evaluated in terms of the interactions between rifampicin and PVA. The hydrophobic nature of rifampicin contributes to impede the complete solvation of the hydrophilic groups of PVA by water molecules. Besides this fact, hydrogen bonding between rifampicin and PVA leads to a hindered effect to the water molecules; therefore, the migration of water is more pronounced in the polymeric matrix, resulting in higher diffusion coefficient.

The effect of the dispersion state of sepiolite on the PVA matrix could be confirmed in PVAS1 sample. The obstruction effect caused by the highly dispersed clay fibers contribute to a slow-mode migration of the water molecules, leading to a decrease of diffusion coefficient. As a fact, PVAS1 shows lower diffusion coefficient and the same X_c of pure PVA. An interesting result is observed to PVAS5. Decreasing diffusion coefficient is expected with both higher clay content and X_c . Nevertheless, 5% of sepiolite leads to highest diffusion coefficient between the samples. Increasing content of sepiolite leads to aggregation of the clay fibers, as observed in WAXS patterns. However, the aggregation state contributes to form preferential water channels by the zeolite-like porous of sepiolite,

resulting in an increasing diffusion coefficient when compared to PVA. Zhang and collaborators have found a similar behavior in poly(acrylic acid-co-acrylamide)/sepiolite nanocomposite hydrogels [26]. In the case of PVAS1R and PVAS5R samples, it seems that the amorphized rifampicin tends to block the access of water molecules to sepiolite pores, leading to a decrease of diffusion coefficient. In order to evaluate the use of the nanocomposite hydrogels for drug release systems, it is necessary a complete understanding of how the presence of both rifampicin and sepiolite changes the swelling capacities and crystallinity of the hydrogels.

4. Conclusions

Nanocomposite hydrogels based on poly(vinyl alcohol) and sepiolite with loaded-rifampicin was successfully prepared. High amounts of sepiolite lead to an increasing degree of crystallinity and to a decrease in swelling capacities. However, the aggregation state of the clay fibers favors the formation of water channels, resulting in higher diffusion coefficient of water. High degree of dispersion was achieved with 1% (w/w) of sepiolite. This fact contributes to diminish the swelling capacity and the water migration into the PVA matrix. The presence of amorphized rifampicin contributes to decrease diffusion coefficient of water and changes the nature of the crystalline domains of PVA. The overall changes on swelling behavior and crystallinity of the nanocomposite hydrogels must be understood in order to evaluate the drug release profile of rifampicin under *in vitro* and *in vivo* conditions.

References

- [1] World Health Organization: Global tuberculosis control: Epidemiology, strategy, financing. WHO, Geneva (2009).
- [2] Sen H., Jindal K. C., Deo K. D., Gandhi K. T.: An improved process for preparation of four-drug anti-tubercular fixed dose combination. WO 200287547 A1, India (2002).
- [3] International Union Against Tuberculosis and Lung Disease: Quality assurance: Protocol for assessing the rifampicin bioavailability of combined formulations in healthy volunteers. The International Journal of Tuberculosis and Lung Disease, 3, s284–s285 (1999).

- [4] Panchagnula R., Agrawal S.: Biopharmaceutic and pharmacokinetic aspects of variable bioavailability of rifampicin. *International Journal of Pharmaceutics*, **271**, 1–4 (2004).
DOI: [10.1016/j.ijpharm.2003.11.031](https://doi.org/10.1016/j.ijpharm.2003.11.031)
- [5] Monkhouse D. C., Lach J. L.: Use of adsorbents in enhancement of drug dissolution I. *Journal of Pharmaceutical Sciences*, **61**, 1430–1435 (1972).
DOI: [10.1002/jps.2600610917](https://doi.org/10.1002/jps.2600610917)
- [6] Monkhouse D. C., Lach J. L.: Use of adsorbents in enhancement of drug dissolution II. *Journal of Pharmaceutical Sciences*, **61**, 1435–1441 (1972).
DOI: [10.1002/jps.2600610918](https://doi.org/10.1002/jps.2600610918)
- [7] Takahashi T., Yamaguchi M.: Host-guest interaction between swelling clay minerals and poorly water-soluble drugs. I: Complex formation between a swelling clay mineral and griseofulvin. *Journal of Inclusion Phenomena and Macrocyclic Chemistry*, **10**, 283–297 (1991).
DOI: [10.1007/BF01066211](https://doi.org/10.1007/BF01066211)
- [8] Takahashi T., Yamaguchi M.: Host-guest interactions between swelling clay minerals and poorly water-soluble drugs: II. Solubilization of griseofulvin by complex formation with a swelling clay mineral. *Journal of Colloid and Interface Science*, **146**, 556–564 (1991).
DOI: [10.1016/0021-9797\(91\)90219-X](https://doi.org/10.1016/0021-9797(91)90219-X)
- [9] Aguzzi C., Cerezo P., Viseras C., Caramella C.: Use of clays as drug delivery systems: Possibilities and limitations. *Applied Clay Science*, **36**, 22–36 (2007).
DOI: [10.1016/j.clay.2006.06.015](https://doi.org/10.1016/j.clay.2006.06.015)
- [10] Santos P. S.: *Clay Technology*, vol 1. (in Portuguese). Edgard Blücher, São Paulo (1975).
- [11] Mehta S. K., Kaur G., Bhasin K. K.: Analysis of Tween based microemulsion in the presence of TB drug rifampicin. *Colloids and Surfaces B: Biointerfaces*, **60**, 95–104 (2007).
DOI: [10.1016/j.colsurfb.2007.06.012](https://doi.org/10.1016/j.colsurfb.2007.06.012)
- [12] Joshi D. P., Lan-Chun-Fung Y. L., Pritchard J. G.: Determination of poly(vinyl alcohol) via its complex with boric acid and iodine. *Analytica Chimica Acta*, **104**, 153–160 (1979).
DOI: [10.1016/S0003-2670\(01\)83825-3](https://doi.org/10.1016/S0003-2670(01)83825-3)
- [13] Tartaglione G., Tabuani D., Camino G.: Thermal and morphological characterisation of organically modified sepiolite. *Microporous and Mesoporous Materials*, **107**, 161–168 (2008).
DOI: [10.1016/j.micromeso.2007.04.020](https://doi.org/10.1016/j.micromeso.2007.04.020)
- [14] Brindley G. W.: X-ray and electron diffraction data for sepiolite. *The American Mineralogist*, **44**, 495–500 (1959).
- [15] Sharma S. K., Nayak S. K.: Surface modified clay/polypropylene (PP) nanocomposite: Effect on physico-mechanical, thermal and morphological properties. *Polymer Degradation and Stability*, **94**, 132–138 (2009).
DOI: [10.1016/j.polyimdegradstab.2008.09.004](https://doi.org/10.1016/j.polyimdegradstab.2008.09.004)
- [16] Yebra-Rodríguez A., Alvarez-Lhoret P., Cardell C., Rodríguez-Navarro A. B.: Crystalline properties of injection molded polyamide-6 and polyamide-6/montmorillonite nanocomposites. *Applied Clay Science*, **43**, 91–97 (2009).
DOI: [10.1016/j.clay.2008.07.010](https://doi.org/10.1016/j.clay.2008.07.010)
- [17] Chen H., Zheng M., Sun H., Jia Q.: Characterization and properties of sepiolite/polyurethane nanocomposites. *Materials Science and Engineering: A*, **445–446**, 725–730 (2007).
DOI: [10.1016/j.msea.2006.10.008](https://doi.org/10.1016/j.msea.2006.10.008)
- [18] Adachi T., Isobe E.: Fundamental characteristics of synthetic adsorbents intended for industrial chromatographic separations. *Journal of Chromatography A*, **1036**, 33–44 (2004).
DOI: [10.1016/j.chroma.2003.09.018](https://doi.org/10.1016/j.chroma.2003.09.018)
- [19] Ricciardi R., Auriemma F., De Rosa C.: Structure and properties of poly(vinyl alcohol) hydrogels obtained by freeze/thaw techniques. *Macromolecular Symposia*, **222**, 49–64 (2005).
DOI: [10.1002/masy.200550405](https://doi.org/10.1002/masy.200550405)
- [20] Agrawal S., Ashokraj Y., Bharatam P. V., Pillai O., Panchagnula R.: Solid-state characterization of rifampicin samples and its biopharmaceutic relevance. *European Journal of Pharmaceutical Sciences*, **22**, 127–144 (2004).
DOI: [10.1016/j.ejps.2004.02.011](https://doi.org/10.1016/j.ejps.2004.02.011)
- [21] Schierholz J. M.: Physico-chemical properties of a rifampicin-releasing polydimethyl-siloxane shunt. *Biomaterials*, **18**, 635–641 (1997).
DOI: [10.1016/S0142-9612\(96\)00071-3](https://doi.org/10.1016/S0142-9612(96)00071-3)
- [22] Ricciardi R., Mangiapia G., Lo Celso F., Paduano L., Triolo R., Auriemma F., De Rosa C., Lauprêtre F.: Structural organization of poly(vinyl alcohol) hydrogels obtained by freezing and thawing techniques: A SANS study. *Chemistry of Materials*, **17**, 1183–1189 (2005).
DOI: [10.1021/cm048632y](https://doi.org/10.1021/cm048632y)
- [23] Ma J., Bilotti E., Peijs T., Darr J. A.: Preparation of polypropylene/sepiolite nanocomposites using supercritical CO₂ assisted mixing. *European Polymer Journal*, **43**, 4931–4939 (2007).
DOI: [10.1016/j.eurpolymj.2007.09.010](https://doi.org/10.1016/j.eurpolymj.2007.09.010)
- [24] Hoffman A. S.: Hydrogels for biomedical applications. *Advanced Drug Delivery Reviews*, **54**, 3–12 (2002).
DOI: [10.1016/S0169-409X\(01\)00239-3](https://doi.org/10.1016/S0169-409X(01)00239-3)
- [25] Crank J.: *Mathematics of diffusion*. Oxford University Press, Oxford (1975).
- [26] Zhang F., Guo Z., Gao H., Li Y., Ren L., Shi L., Wang L.: Synthesis and properties of sepiolite/poly(acrylic acid-co-acrylamide) nanocomposites. *Polymer Bulletin*, **55**, 419–428 (2005).
DOI: [10.1007/s00289-005-0458-2](https://doi.org/10.1007/s00289-005-0458-2)